Spiral spin state with open boundary conditions in a magnetic field

Randy S. Fishman and Satoshi Okamoto
Materials Science and Technology Division, Oak Ridge National Laboratory, Oak Ridge, Tennessee 37831, USA
(Received 24 April 2017; revised manuscript received 22 June 2017; published 28 July 2017)

In order to model a spiral spin state in a thin film, we study a classical Heisenberg model with open boundary conditions. With magnetic field applied in the plane of the film, the spin state becomes ferromagnetic above a critical field that increases with thickness N. For a given N, the spiral passes through states with $n = n_0$ up to 0 complete periods in steps of 1. These numerical results agree with earlier analytic results in the continuum limit and help explain the susceptibility jumps observed in thin films.

DOI: 10.1103/PhysRevB.96.014439

I. INTRODUCTION

Due to its close connection with multiferroic behavior, spiral spin order [1,2] such as in Fig. 1 has been the subject of intense investigation. Recently, spiral order was discovered [3–9] in several thin films. In order to manipulate the magnetic properties of these spiral states, it is essential to understand how they depend on film thickness N and magnetic field B. A spiral in a thin film can be modeled by a linear Heisenberg model with neighboring spins coupled by a ferromagnetic interaction J and by a Dzyaloshinskii-Moriya (DM) interaction D [10,11] due to broken inversion symmetry.

In the bulk limit, this simple model has an analytic solution that supports solitonic states [12]. Consequently, the spiral state is often referred to as a "solitonic" lattice. For thin films, this model is believed to describe materials like $Cr_{1/3}NbS_2$ [4,6,9] and MnSi [5]. In $Cr_{1/3}NbS_2$, Togawa *et al.* [9] directly imaged the "solitonic lattice" by Lorentz microscopy in a 1-μm-thick sample. They also found that the spiral state produces steps in the magnetoresistance versus field, applied perpendicular to the chiral axis or in the plane of the spiral. In MnSi [5], the spiral was detected both in magnetoresistance measurements and in the magnetization versus applied field for 25- and 30-nm-thick samples.

For both materials, measurements exhibit discontinuous changes as the number n of periods of the spiral decreases by one with increasing field. A high enough field stabilizes a ferromagnetic state with $n = 0$ so that all spins point along the field direction. Because the chirality of the spiral is maintained against defects and temperature, thin films that support spiral states have been considered as magnetic storage devices [13].

To understand the behavior of a spiral sandwiched between two other magnetic materials, the model described above has been studied [14] with fixed boundary conditions so that the spins $\mathbf{S}_i$ on sites $i = 1$ and N are fixed along the field direction perpendicular to the chiral axis. However, most thin films may be better described using open boundary conditions so that the end spins are free to rotate. For example, both the $Cr_{1/3}NbS_2$ and MnSi samples discussed above were grown on magnetically inert Si wafers.

Our numerical solution of this problem qualitatively agrees with an earlier analytic solution [5] in the continuum limit. We predict that thin films will exhibit jumps in the magnetization and peaks in the susceptibility when n decreases by one with increasing field. Remarkably, our results are also quite similar to earlier results that imposed fixed boundary conditions [14].

II. MODEL AND THEORETICAL RESULTS

The Hamiltonian for this problem is

$$\mathcal{H} = -J\sum_{i=1}^{N-1}\mathbf{S}_i\cdot\mathbf{S}_{i+1} - D\sum_{i=1}^{N-1}\mathbf{z}\cdot(\mathbf{S}_i\times\mathbf{S}_{i+1}) + A\sum_{i=1}^{N}(\mathbf{z}\cdot\mathbf{S}_i)^2 - 2\mu_B B\sum_{i=1}^{N}\mathbf{x}\cdot\mathbf{S}_i, \quad (1)$$

where the spins $\mathbf{S}_i$ are treated classically and interact with their neighbors through the ferromagnetic exchange J and the DM interaction D. The anisotropy $A > 0$ keeps the spins in the xy plane. Notice that the end spins at sites $i = 1$ and N are treated differently than spins in the interior. For example, the spin at $i = N$ experiences an exchange interaction with the spin at $i = N - 1$ but the spin at $N + 1$ is missing. All spins experience the same magnetic field along $\mathbf{x}$ in the plane of the film.

The dimensionless parameters of this model are $d \equiv D/J$ and $b \equiv 2\mu_B B/JS$. Aside from keeping all the spins $\mathbf{S}_i = S(\cos\theta_i, \sin\theta_i, 0)$ in the xy plane, the anisotropy A has no affect on the static properties of this model. For a bulk system ($N \to \infty$), the DM interaction produces a spiral with wavelength $\Lambda = 2\pi/\tan^{-1}(d) \approx 2\pi/d$. When $d > 0$, the spiral is right handed; when $d < 0$, it is left handed.

Starting with a uniform spiral, the spin state is allowed to relax in discrete time steps. At each step, we obtain updated values for the spins from the condition that $\mathbf{S}_i$ lies along the effective field $\mathbf{h}_i$, where the energy at site i is given by $-JS\mathbf{h}_i\cdot\mathbf{S}_i$. The dimensionless effective field $\mathbf{h}_i$ has components

$$h_{ix} = \cos\theta_{i+1} + \cos\theta_{i-1} + d(\sin\theta_{i+1} - \sin\theta_{i-1}) + b, \quad (2)$$

$$h_{iy} = \sin\theta_{i+1} + \sin\theta_{i-1} - d(\cos\theta_{i+1} - \cos\theta_{i-1}). \quad (3)$$

Of course, $h_{iz} = 0$. For the end spins at $i = 1$ or N, the exchange and DM terms to the left ($i = 0$) or the right ($i = N + 1$) are missing.

Approximately 90% of the old state is mixed with 10% of the new state in order to avoid oscillations between possible solutions. This procedure continues until no further updates are obtained. In order to simplify this procedure, we use the fact that the spin state is either mirror symmetric about the center for even N or has spin angle $\theta_i = 0$ or π at the central site for odd N. These symmetry considerations reduce the number of spin degrees of freedom by half. Even for the largest thickness

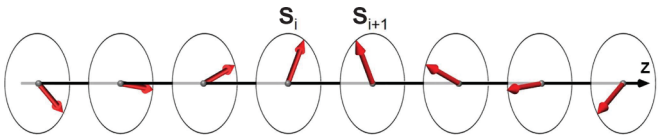

FIG. 1. A spiral spin state propagating along **z**. The thin film has dimensions $M \times M \times N$, where N is the thickness and $M \gg N$.

$N = 250$ in Fig. 1, our numerical procedure converges in less than 10^5 steps. To locate the phase boundary between different topological sectors, we compare the energy of different sectors. Only during the field sweep within each topological sector, we used a lower-field solution as an initial trial state to accelerate the convergence.

To evaluate the phase diagram, we take $d = 0.16$, which corresponds to a zero-field spiral with wavelength $\Lambda = 39.6$, the same as observed in bulk $Cr_{1/3}NbS_2$ [4]. Phase boundaries

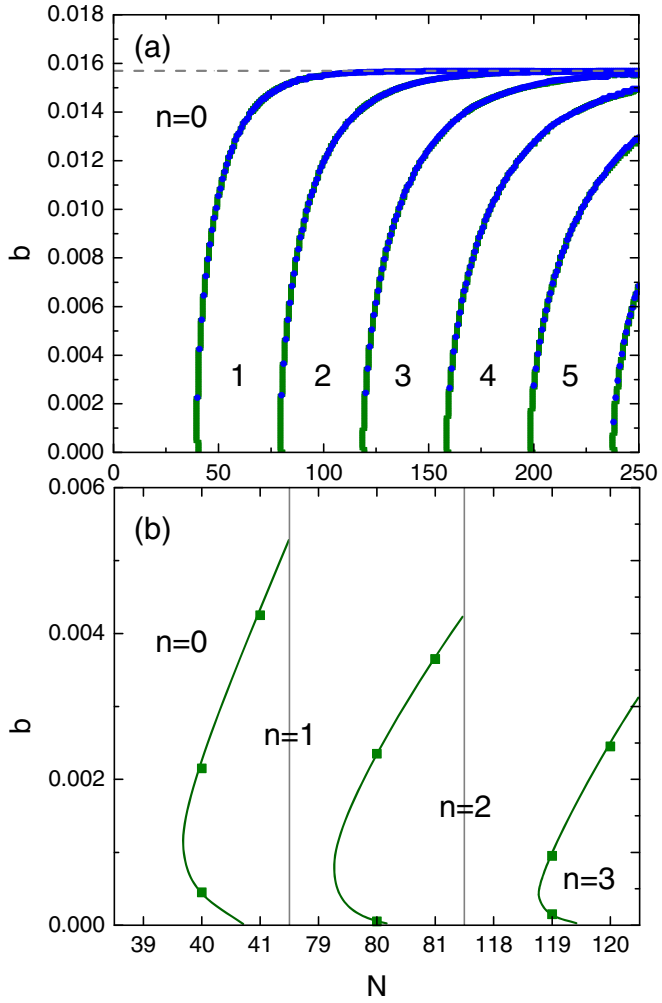

FIG. 2. Phase diagram of spiral spin state with dimensionless DM interaction $d = 0.16$. Plots show dimensionless magnetic field b versus thickness N. The number of complete periods of the spiral is n. (a) Green squares were evaluated by sweeping the thickness, and blue circles by sweeping the magnetic field. The horizontal dashed line shows $b_c \approx (\pi/4)^2 d^2 = 0.0157$ [12]. (b) Square points separate regions with different values of N at the phase boundaries.

are evaluated by either sweeping in thickness N for a fixed magnetic field or in magnetic field b for a fixed thickness. As seen in Fig. 2(a), these two techniques produce consistent results.

In zero field, the spiral is not affected by the open boundary conditions because the rotation angle $\phi = \cos^{-1}(\mathbf{S}_i \cdot \mathbf{S}_{i+1}/S^2)$ does not change between pairs of spins at sites i and $i+1$, even for the first and last pairs with $i = 1$ and $N-1$. Hence, the zero-field spiral has the bulk period $\Lambda = 39.6$. The transition from $n = n'$ to $n' + 1$ complete periods occurs when $N - 1$ just exceeds $(n' + 1)\Lambda$. So in zero field, the ferromagnetic state ($n' = 0$) is stable below $N = 41$.

In nonzero field, the end sites behave differently than the interior sites because the effective fields $\mathbf{h}_1$ and $\mathbf{h}_N$ at sites $i = 1$ and N contain only half the exchange and DM couplings from their neighbors but the full magnetic field $b\mathbf{x}$. This difference quantizes the number of periods n of the spiral.

For any thickness, the spiral passes through states with $n = n_0$ to 0 complete periods in steps of 1 as b increases. At high thicknesses ($N \gg \Lambda$), the ferromagnetic state is stable above $b_c \approx (\pi/4)^2 d^2 = 0.0157$ [12]. These results agree with earlier calculations [5] made in the continuum limit and with previous results [14] that assumed fixed boundary conditions.

The spin $\cos\theta_i$ along the field direction is plotted as a function of i in Fig. 3 for $b = 0.01$. The pairs of thicknesses in Figs. 3(a) and 3(b) were chosen so that the spiral passes from $n = n'$ to $n = n' + 1$ with increasing N. In a nonzero magnetic field, the spin state becomes anharmonic with the spins $\mathbf{S}_i$ spending more time with $\cos\theta_i > 0$ than with $\cos\theta_i < 0$ as they rotate about **z**. As a result, $\cos\theta_i$ is more rounded near $\cos\theta_i = 1$ and sharper near $\cos\theta_i = -1$. For the end spins, $\cos\theta_i$ always increases just above the phase boundary.

Surprisingly, each phase boundary in Fig. 2(a) exhibits a slight bulge toward lower N with increasing field. This behavior is shown in Fig. 2(b). Hence, the boundary between 0 and 1 node is 40.5 at zero field but drops to 39.5 at $b = 0.001$. A value of 40.5 is recovered at $b = 0.003$. The bulge moves to lower fields with increasing N. Its presence implies that a state with $n = n'$ complete periods at zero field can transform into a state with $n = n' + 1$ before n starts to decrease with increasing field. To better understand this behavior, we plot the spin configuration for $N = 119$ for fields b ranging from

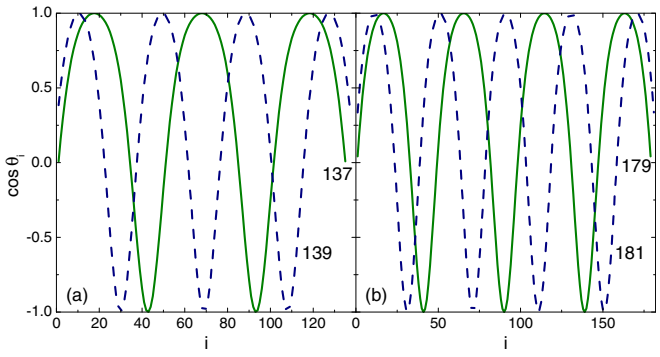

FIG. 3. Spin along the field direction as a function of site i for different thicknesses and $b = 0.01$. In (a), $N = 137$ and 139 correspond to $n = 2$ and 3, respectively. In (b), $N = 179$ and 181 correspond to $n = 3$ and 4, respectively.

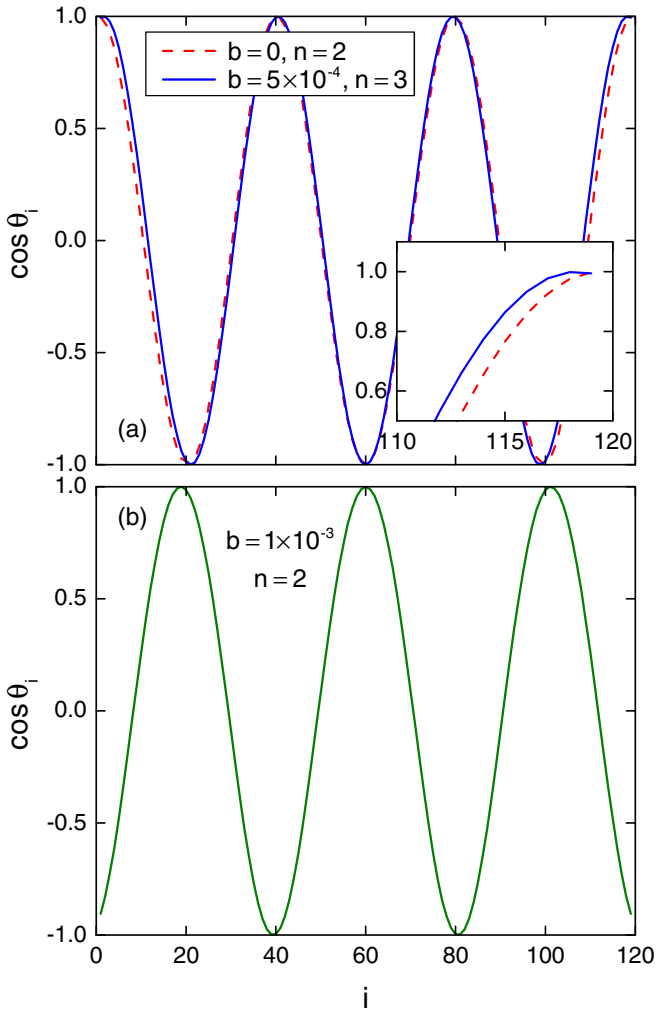

FIG. 4. Spin along the field direction as a function of site i for $N = 119$ and (a) $b = 0$ and 0.0005, and (b) $b = 0.001$. Starting with $n = 2$ complete periods at $b = 0$, the spin configuration changes to $n = 3$ at $b = 0.0005$ and back to $n = 2$ at $b = 0.001$. The increase in n in (a) is produced by the downturn in $\cos\theta_i$ at the end sites, as shown in the inset.

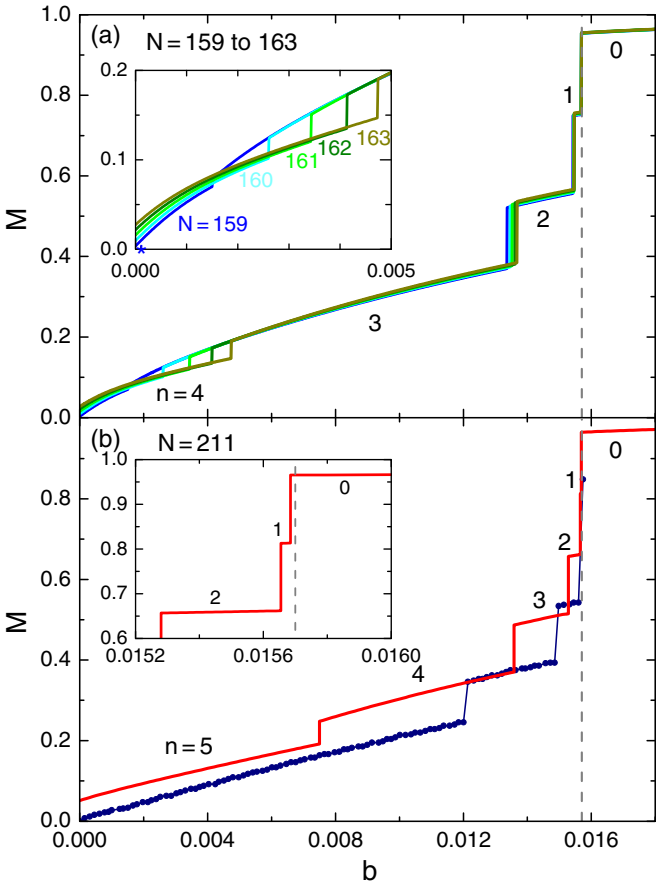

FIG. 5. Average magnetization as a function of magnetic field for thicknesses $N = 159$–163 (a) and $N = 211$ (b). The vertical dashed line shows $b_c = 0.0157$ [12]. Circles in (b) are the numerical results with the fixed boundary condition taken from Ref. [14]. The inset of (a) shows the jump from $n = 4$ to 3 for each thickness N. The inset of (b) shows the jumps from $n = 2$ to 0.

0 to 0.001 in Fig. 4. Although the number of complete periods n increases from 2 to 3 from $b = 0$ to 0.0005, the spin configuration is continuous. On the other hand, the spin configuration changes discontinuously (with $\cos\theta_i$ changing from -1 to 1 at the central site $i = 60$) as the field increases from $b = 0.0005$ to 0.001 and n decreases from 3 back to $n = 2$. So the "reentrance" in Fig. 2 is only a mathematical oddity and the lower transition has no physical effect.

Keeping the thickness fixed, we plot the average magnetization

$$M = \frac{1}{N}\sum_{i=1}^{N}\cos\theta_i \tag{4}$$

versus magnetic field b in Fig. 5. As b increases, the magnetization jumps when n drops by one. Those jumps become larger as n approaches 0. For thicknesses $N = 159$–163, the spiral has three periods over the largest range of magnetic field. Above b_c, the magnetization depends very weakly on field and continues to saturate as b increases. A close examination reveals M is continuous at the "reentrant" transition for $N = 159$ from $n = 3$ to 4 at $b \approx 10^{-4}$, indicated by the star in the inset in Fig. 5(a).

We found that the boundary condition influences the low field behavior rather strongly. Figure 5(b) compares two results for $N = 211$ with different boundary conditions. Circles are the results of the fixed boundary condition, in which the direction of boundary spins is fixed along the field direction (taken from Ref. [14]), and the solid line is the result with the free boundary condition (current work). Because boundary spins can move freely, the spin configuration can be modified more easily under a magnetic field. As a result, low-field magnetization is slightly enhanced, and the phase boundaries between different topological sectors are shifted to lower fields. This implies that the phase boundaries are more rounded in Fig. 2(a) than those with the fixed boundary condition. Nevertheless, the critical field, above which the $n = 0$ sector is most stable, is not changed.

Experimentally, a thin film will exhibit susceptibility peaks at the field separating $n' + 1$ from n' spiral periods. For very thin films, there may be only one or two peaks. For larger films,

several peaks may be observable. However, the peaks will be largest as n approaches 0. For films with $N-1$ below the spiral period Λ, the susceptibility will be a smooth function of field.

Because an actual film contains steps, its properties are averaged over several thicknesses N. These steps then smear out the susceptibility peaks. Nonetheless, Wilson *et al.* [5] successfully observed two susceptibility peaks in a MnSi film. Presumably, the lower peak marks the transition from $n=2$ to 1 and the higher, larger peak from $n=1$ to 0.

The insensitivity of the phase diagram of this model to the precise boundary conditions is remarkable. Open boundary conditions seem just as effective at quantizing the number of spiral periods as fixed boundary conditions. Qualitatively, a phase diagram like that in Fig. 2 requires only that the end spins are treated differently than the interior spins. Of course, the details of the phase diagram, such as the critical fields for the transitions from $n=n'$ to $n'-1$ for a fixed N, will depend on the specific boundary conditions.

III. SUMMARY

To conclude, we have evaluated the magnetic state and phase diagram of a spiral with open boundary conditions. For every thickness, the spin state passes through every number of complete periods from n_0 to 0 with increasing field. A decrease in n by one is marked by a jump in the magnetization and by a peak in the magnetic susceptibility. Most importantly, the qualitative behavior of spiral states in thin films does not depend on the precise boundary conditions.

ACKNOWLEDGMENTS

We acknowledge helpful conversations with Zheng Gai. Research was sponsored by the US Department of Energy, Office of Science, Office of Basic Energy Sciences, Materials Sciences and Engineering Division.

This manuscript has been authored by UT-Battelle, LLC under Contract No. DE-AC05-00OR22725 with the U.S. Department of Energy. The United States Government retains and the publisher, by accepting the article for publication, acknowledges that the United States Government retains a nonexclusive, paid-up, irrevocable, worldwide license to publish or reproduce the published form of this manuscript, or allow others to do so, for United States Government purposes. The Department of Energy will provide public access to these results of federally sponsored research in accordance with the DOE Public Access Plan (http://energy.gov/downloads/doe-public-access-plan).

[1] D. I. Khomskii, J. Magn. Magn. Mater. **306**, 1 (2006).
[2] S.-W. Cheong and M. Mostovoy, Nat. Mater. **6**, 13 (2007).
[3] W. Z. Wang, K. L. Yao, and H. Q. Lin, J. Chem. Phys. **112**, 487 (2000).
[4] Y. Togawa, T. Koyama, K. Takayanagi, S. Mori, Y. Kousaka, J. Akimitsu, S. Nishihara, K. Inoue, A. S. Ovchinnikov, and J. Kishine, Phys. Rev. Lett. **108**, 107202 (2012).
[5] M. N. Wilson, E. A. Karhu, D. P. Lake, A. S. Quigley, S. Meynell, A. N. Bogdanov, H. Fritzsche, U. K. Rossler, and T. L. Monchesky, Phys. Rev. B **88**, 214420 (2013).
[6] B. J. Chapman, A. C. Bornstein, N. J. Ghimire, D. Mandrus, and M. Lee, Appl. Phys. Lett. **105**, 072405 (2014).
[7] S. A. Meynell, M. N. Wilson, H. Fritzsche, A. N. Bogdanov, and T. L. Monchesky, Phys. Rev. B **90**, 014406 (2014).
[8] N. A. Porter, C. S. Spencer, R. C. Temple, C. J. Kinane, T. R. Charlton, S. Langridge, and C. H. Marrows, Phys. Rev. B **92**, 144402 (2015).
[9] Y. Togawa, T. Koyama, Y. Nishimori, Y. Matsumoto, S. McVitie, D. McGrouther, R. L. Stamps, Y. Kousaka, J. Akimitsu, S. Nishihara, K. Inoue, I. G. Bostrem, Vl. E. Sinitsyn, A. S Ovchinnikov, and J. Kishine, Phys. Rev. B **92**, 220412 (2015).
[10] I. E. Dzyaloshinskii, J. Exp. Theor. Phys. (USSR) **37**, 881 (1959); Sov. Phys.–JETP **10**, 628 (1960).
[11] T. Moriya, Phys. Rev. **120**, 91 (1960).
[12] J. Kishine, K. Inoue, and Y. Yoshida, Prog. Theor. Phys. **159**, 82 (2005).
[13] H.-B. Braun, J. Kulda, B. Roessli, D. Visser, K. W. Krämer, H.-L. Güdel, and P. Böni, Nat. Phys. **1**, 159 (2005).
[14] J.-I. Kishine, I. G. Bostrem, A. S. Ovchinnikov, and Vl. E. Sinitsyn, Phys. Rev. B **89**, 014419 (2014).